FLOW FIELD COMPUTATIONAL ANALYSIS IN A SOLID FUEL RAMJET COMBUSTOR

Hélio de Miranda Cordeiro
Instituto de Pesquisa e Desenvolvimento – GQ/IPD
23010-470 – Guaratiba, RJ, Brazil
hcordeir@ipd.eb.mil.br

Angela Ourivio Nieckele
Department of Mechanical Engineering, Pontifical Catholic University of Rio de Janeiro
22453-900 – Rio de Janeiro, RJ, Brazil
nieckele@mec.puc-rio.br

Abstract. *Numerical analysis of reactive and turbulent flow field in a solid fuel ramjet combustor. The ability of different models to predict solid fuel pyrolysis is investigated. The mathematical model is based on the numerical solution of the conservation equations of mass, momentum, energy and transport equations for scalar quantities. The* κ–ε *turbulence model for high Reynolds is employed and the combustion is modeled with the mixture fraction/prescribed probability density function formalism. Close to the walls a law-of-the-wall is specified, with the boundary layer divided into two regions, a viscous sub layer and a fully turbulent region. Heat and mass transfer at the walls are calculated using a modified law-of-the-wall based on a blowing parameter. The results, obtained using the proposed model, are compared with others earlier models predictions and with empirical data. It was verified that the results are in good agreement with literature data, allowing the conclusion that the model presented is suitable for the prediction of the mass transfer and flow field in a solid fuel ramjet combustor.*

Keywords*. Combustion, solid fuel, ramjet, computational analysis*

1. Introduction

The ramjet with subsonic combustion is considered the simplest and hence the most reliable and the least expensive propulsion device for supersonic flight. The solid fuel ramjet (SFRJ) has been used for the propulsion of tactical missiles and gun-launched projectiles. In these applications there is another propulsion system that launches the ramjet at supersonic speed. Figure (1) shows the typical configuration of solid fuel ramjet. This typical configuration consists of an air intake, an exhaust nozzle and a combustor. The combustor includes the solid fuel chamber combustion and the aft mixing chamber.

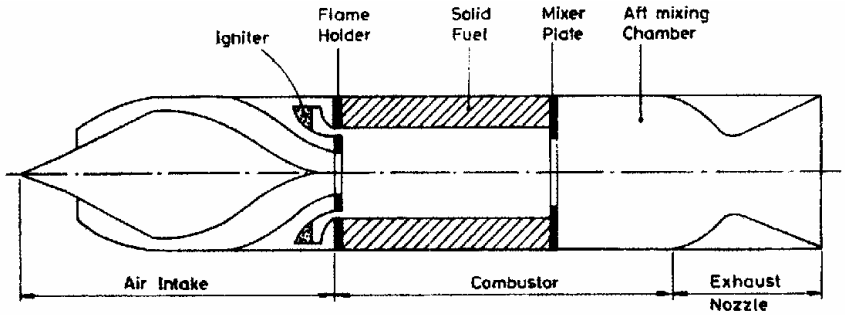

Figure 1. Typical configuration of a solid fuel ramjet.

The operation of the solid fuel ramjet can be summarized as follow. First, at the air intake, the air passage through supersonic diffuser yields a shockwave, consequently the temperature and pressure increase. The heated air and the high pressure promote the solid fuel pyrolysis in the combustor. Gaseous products at high temperature are expanded through nozzle yielding thrust. The objective of this paper is to present a mathematical model used in a computational simulation of a turbulent and reacting flow field within a solid fuel ramjet combustor. The simulation yields information about velocity, temperature and scalar variables flow field. The solid fuel regression rate at the solid fuel wall is also estimated.

2. The mathematical model

The flow was assumed to be subsonic, two-dimensional and steady, that is, transient effects were neglected. The viscous work was neglected since low Mach number flow approach was used. Soret and Dufour effects were neglected such as radiant heat transfer.

The mathematical model is based on the solution of the Favre-averaged conservation equations for mass, momentum, energy and transport equations for scalar quantities. Two parameters turbulence model (Launder and Spalding, 1976) was employed to calculate effective viscosity using the formulas.

$$\mu_{eff} = \mu + \mu_t \tag{1}$$

$$\mu_t = C_\mu \, \bar{\rho} \, \kappa^2 / \varepsilon \tag{2}$$

where C_μ is an empirical constant, $\bar{\rho}$ is the mean gas density, μ_t is the turbulent viscosity and μ is the laminar viscosity being $\mu_t >> \mu$. Equation (2) requires that two additional transport equations (for turbulence kinetic energy, κ, and its dissipation rate, ε) be evaluated. The governing equations are presented below.

$$\frac{\partial}{\partial x_i}(\bar{\rho}\tilde{u}_i) = 0 \tag{3}$$

$$\frac{\partial}{\partial x_j}(\bar{\rho}\tilde{u}_j\tilde{u}_i) = \frac{\partial}{\partial x_j}\left(\mu_t \frac{\partial \tilde{u}_i}{\partial x_j}\right) + \frac{\partial}{\partial x_j}\left(\mu_t \frac{\partial \tilde{u}_j}{\partial x_i}\right) - \frac{\partial \bar{P}}{\partial x_i} \tag{4}$$

$$\frac{\partial}{\partial x_j}(\bar{\rho}\tilde{u}_j\tilde{H}) = \frac{\partial}{\partial x_j}\left[\frac{\mu_t}{\sigma_t}\left(\frac{\partial \tilde{H}}{\partial x_j}\right)\right] \tag{5}$$

$$\frac{\partial}{\partial x_j}(\bar{\rho}\tilde{u}_j\kappa) = \frac{\partial}{\partial x_j}\left[\frac{\mu_t}{\sigma_k}\frac{\partial \kappa}{\partial x_j}\right] + P_\kappa - \bar{\rho}\varepsilon \tag{6}$$

$$\frac{\partial}{\partial x_j}(\bar{\rho}\,\tilde{u}_j\varepsilon) = \frac{\partial}{\partial x_j}\left[\frac{\mu_t}{\sigma_\varepsilon}\frac{\partial \varepsilon}{\partial x_j}\right] + C_1\frac{\varepsilon}{\kappa}P_\kappa - C_2\bar{\rho}\frac{\varepsilon^2}{\kappa} \tag{7}$$

where $\tilde{u}_i$ and $\tilde{u}_j$ are mean velocity components, $\bar{P} = \bar{p} + (2/3)[(\mu_t \, \partial \tilde{u}_k / \partial x_k) + (\bar{\rho}\kappa)]$ is a modified pressure, $\bar{p}$ is the combustor mean pressure, $\tilde{H}$ is the mean stagnation enthalpy given by $\tilde{H} = \tilde{h} + \tilde{u}_i\tilde{u}_i/2 + \kappa$, $\tilde{h}$ is the mean specific enthalpy and P_κ is the turbulent kinetic energy production term defined by

$$P_k = -\overline{\rho u_i'' u_j''}\frac{\partial \tilde{u}_i}{\partial x_j} = \mu_t\left(\frac{\partial \tilde{u}_i}{\partial x_j} + \frac{\partial \tilde{u}_j}{\partial x_i}\right)\frac{\partial \tilde{u}_i}{\partial x_j} - \frac{2}{3}\left[\mu_t\left(\frac{\partial \tilde{u}_k}{\partial x_k}\right) + \bar{\rho}\,\kappa\right]\frac{\partial \tilde{u}_i}{\partial x_j}\delta_{ij} \tag{8}$$

The empirical constants of the model are C_1=1.43, C_2=1.92, C_μ=0.09, σ_t =0.7; σ_κ=1.0 and σ_ε=1.3 (Launder and Spalding, 1973).

Combustion is modeled using the conserved scalar/presumed probability density function (p.d.f.) formalism. It is assumed that combustion is described by a single one-step irreversible reaction between the fuel and the oxidizer yielding combustion products. Therefore the combustion process is mixing limited. This assumption provides relationships between the instantaneous values of chemical species concentrations and the conserved scalar, taken as the mixture fraction.

The mean values of the species mass fraction and gas mixture temperature may be found from

$$\tilde{\phi} = \int_0^1 \phi(f)\,p(f)\,df \tag{9}$$

where $\tilde{\phi}$ is the variable mean value, $\phi(f)$ is the variable instantaneous value, $p(f)$ is the probability density function and f is the mixture fraction. When the variable is mass fraction, $\phi(f)$ is obtained from state relationships. The instantaneous gas mixture temperature is function of mixture enthalpy and mixture fraction. Therefore, instantaneous gas mixture temperature is given by $\phi(f, h)$.

The p.d.f. was defined using normalized Beta function (Wolfram, S. 2002)

$$p(f) = \frac{f^{a-1}(1-f)^{b-1}}{\int_0^1 f^{a-1}(1-f)^{b-1}\,df} \tag{10}$$

where the parameters a and b are completely defined in terms of the mean value of the mixture fraction, $\tilde{f}$, and its variance, g_f, as

$$a = \tilde{f}\left[\frac{\tilde{f}(1-\tilde{f})}{g_f} - 1\right] \tag{11}$$

$$b = \frac{a(1-\tilde{f})}{\tilde{f}} \tag{12}$$

Favre-averaged transport equations are solved to compute $\tilde{f}$ and g_f,

$$\frac{\partial}{\partial x_i}\left(\bar{\rho}\ \tilde{u}_i\ \tilde{f}\right) = \frac{\partial}{\partial x_i}\left(\frac{\mu_t}{\sigma_f}\frac{\partial \tilde{f}}{\partial x_j}\right) \tag{13}$$

$$\frac{\partial}{\partial x_j}(\bar{\rho}\tilde{u}_j g_f) = \frac{\partial}{\partial x_j}\left(\frac{\mu_t}{\sigma_t}\frac{\partial g_f}{\partial x_j}\right) - 2\frac{\mu_t}{\sigma_t}\left(\frac{\partial \tilde{f}}{\partial x_j}\right)^2 - 2\bar{\rho}\frac{\varepsilon}{\kappa}g_f \tag{14}$$

The mean gas density was calculated using the equation of state

$$\bar{\rho} = \frac{\bar{p}}{\Re \tilde{T}}\frac{1}{\sum_j \frac{\tilde{m}_j}{M_j}} \tag{15}$$

where $\Re$ is the universal gas constant, M_j is the molecular mass of j specie and $\tilde{T}$ is the mean gas mixture temperature.

3. Geometry and boundary conditions

Figure (2) shows schematically a simplified geometry of the combustor. It does not present a step after the fuel grain. The geometric parameters are: the inlet radius $R_{in,}$ the outlet radius R, the combustor length L and the fuel length $X_{fuel.}$ The partial differential equations can be solved if the required boundary conditions are specified. At the inlet was assumed uniform distribution for all variables. At the outlet and the centerline of the combustor, a no-gradient condition was used for all equations except the r-momentum equation for which a zero velocity is specified. All solid boundaries present no slip condition (both velocity components equal to zero), in addition, were considered adiabatic and impermeable except the solid fuel surface where mass injection (also called blowing) occurs due to fuel regression.

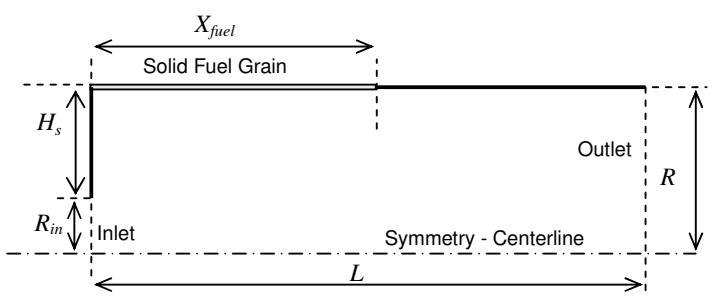

Figure 2. Geometric parameters of computational domain.

3.1 Adiabatic and impermeable walls

In this case, diffusive flux through the walls for $\tilde{H}$, $\tilde{f}$ and g_f variables were considered equal to zero. Near solid walls, viscous effects become important due to no slip condition. Thus, κ–ε turbulence model is not valid close to the walls, where Reynolds number is low.

For simplicity, a two-region boundary layer was used. The border between the laminar sub layer and the fully turbulent layer was taken at y^+=11.5. This dimensionless variable was defined by

$$y^+ = \frac{\bar{\rho}\ y_P\ (\tau_w / \bar{\rho})^{1/2}}{\mu} \tag{16}$$

where y_p is the near-wall node distance from the wall, τ_w is the wall shear stress and $\overline{\rho}$ is evaluated at y_p. The fully turbulent region is taken at $y^+ \geq 11.5$.

Defining a dimensionless axial velocity by $u^+ = \tilde{u}_P / \sqrt{\tau_w / \overline{\rho}}$, for stationary and two-dimensional boundary layer without gradient pressure and blowing or suction, the following equations can be used near the wall region:

$$\text{If} \quad y^+ \geq 11.5 \qquad \text{then} \quad u^+ = \frac{1}{k} \ln (E\, y^+) \tag{17}$$

$$\text{If} \quad y^+ < 11.5 \qquad \text{then} \quad u^+ = y^+ \tag{18}$$

where $k = 0.4$ is the von Kárman constant and $E \approx 9.0$. The Eq. (16-18) are used to compute wall shear stress given by

$$\text{If} \quad y^+ \geq 11.5 \qquad \text{then} \qquad \tau_w = \frac{\tilde{u}_P\, y_P^+\, \mu / y_P}{(1/k) \ln (E\, y_P^+)} \tag{19}$$

$$\text{If} \quad y^+ < 11.5 \qquad \text{then} \qquad \tau_w = \frac{\tilde{u}_P\, \mu}{y_P} \tag{20}$$

In the fully turbulent region, it was assumed equilibrium between the production and the destruction of turbulent kinetic energy. As a consequence, turbulent kinetic energy is proportional to the wall shear stress, which is approximately constant in the near wall region. Therefore, the following equations were applied to calculate the turbulent kinetic energy and its dissipation rate at the near wall region, where the subscript P means first internal node point.

$$\partial \kappa / \partial y = 0 \tag{21}$$

$$\varepsilon_P = \frac{C_\mu^{3/4} \kappa_P^{3/2}}{k\, y_P} \tag{22}$$

3.2 Solid fuel surface

The pyrolizing fuel causes a mass flux of fuel from the wall to the main flow, where the fuel is burnt. The blowing velocity can be evaluated from

$$v_w = \frac{\dot{q}_w}{\overline{\rho}_{fu-g} H_{v,eff}} \tag{23}$$

where $\dot{q}_W$ is heat flux to the wall, $\overline{\rho}_{fu-g}$ is the density of gaseous fuel and $H_{v,eff}$ is the effective heat of gasification, i.e., the amount of heat required to pyrolize 1 kg of fuel. Because of the blowing velocity, the wall functions early presented cannot be used, and a modified wall function is used to account for the blowing effects.

The assumptions employed for reacting flows result in then following general boundary condition for all "conserved" variables (ϕ_c) on a surface which has mass transfer (Kays, 1966)

$$\dot{m}''_{bw} = \left(\Gamma_{\phi_c} \frac{\partial \phi_c}{\partial r} \right)_{bw} / (\phi_{c,bw} - \phi_{c,fg}) \tag{24}$$

where $\dot{m}''_{bw}$ is mass flux by the wall, the subscripts *bw* (*blowing wall*) e *fg* (*fuel grain*) refer to surface and inner solid fuel values, respectively, and Γ_{ϕ_c} is the effective transport coefficient of conserved variable (stagnation enthalpy or mixture fraction).

A mass transfer conductance (g) is often defined such that

$$\left(\Gamma_{\phi_c} \frac{\partial \phi_c}{\partial r} \right)_{bw} = g\, (\phi_{cP} - \phi_{c,bw}) \tag{25}$$

where ϕ_{cP} is near-wall value. From Eq. (25) into Eq. (24) yields

$$\dot{m}''_{bw} = g\ (\phi_{c_P} - \phi_{c,bw})/(\phi_{c,bw} - \phi_{c,fg}) = gBP \tag{26}$$

where BP represents the mass transfer parameter (or blowing parameter). In this application, BP was evaluated from the solution of energy equation using

$$BP = (\tilde{H}_P - \tilde{H}_{bw})/(\tilde{H}_{bw} - \tilde{H}_{fg}) \tag{27}$$

Using Reynolds analogy and Couette flow approximation for the boundary layer behavior with mass transfer, the following expression can be found (Kays, 1966)

$$\tau_{bw} = \tau_w \ \mathbf{ln}(1 + BP)/BP \tag{28}$$

where τ_{bw} is wall shear stress with mass transfer and τ_w is wall shear stress calculated from Eq. (19) or Eq. (20).

Since the blowing rates were small for the solid fuel ramjet, the boundary conditions for κ, ε and g_f used at the adiabatic and impermeable walls also can be employed in blowing wall situations. The boundary condition for scalar conservative variable was evaluated from

$$\left(\Gamma_{\tilde{H}} \frac{\partial \tilde{H}}{\partial r}\right)_{bw} = \frac{\tau_{bw}}{\tilde{u}_P}(\tilde{H}_P - \tilde{H}_{bw}) \quad \text{and} \quad \left(\Gamma_{\tilde{f}} \frac{\partial \tilde{f}}{\partial r}\right)_{bw} = \frac{\tau_{bw}}{\tilde{u}_P}(\tilde{f}_P - \tilde{f}_{bw}) \tag{29}$$

The mean local regression rate can be evaluated from

$$\dot{r} = \frac{\dot{q}_w}{\overline{\rho}_{fu-s} H_{v,eff}} = \frac{H_{v,eff}\overline{\rho}_{fu-g} v_w}{\overline{\rho}_{fu-s} H_{v,eff}} \Rightarrow \dot{r} = \frac{\overline{\rho}_{fu-g}}{\overline{\rho}_{fu-s}} v_w \tag{30}$$

where $\overline{\rho}_{fu-s}$ is the solid fuel density.

4. Solution procedures

The governing equations were integrated in each control volume using a finite-volume method (Patankar, 1980). The equations were discretized using the power-law scheme. The discretized set of equations was solved by means of the iterative procedure (TDMA algorithm line by line) (Patankar, 1980) using the block correction algorithm (Settari & Aziz, 1973) and under relaxation to promote convergence. The iterations are important since the equations are coupled and nonlinear. A staggered grid system was used in which the velocity components were stored at the boundaries of the control volume for the other variables. Pressure-velocity coupling was accomplished by means of the SIMPLE algorithm (Patankar, 1980).

5. Results and discussion

At this section, two cases are presented. The first case aims to validate the methodology and numerical code employed by analyzing the flow of heated air through a pipe with a sudden expansion at the inlet. The second case presents the results obtained with the proposed computational model. The flow field inside a solid fuel combustion chamber of a ramjet is investigated. The results were compared with available experimental and numerical data presented in the early papers.

5.1 Turbulent flow through a sudden pipe expansion

This case consists of a sudden pipe expansion, without combustion. It was used for validation purpose of the numerical code by analyzing the velocity and temperature flow fields. The length of the pipe is 1 m, the diameter downstream of the expansion is 0.2 m and the inlet diameter is 0.1 m. Calculations were performed based on the air flow with temperature equal to 650 K and Reynolds number equal to 4×10^5 (based on the inlet diameter and mean inlet velocity).

The results were obtained using a non-uniform computational grid with 82×62 grid nodes shown in the Fig. (3) above. There is a strong grid concentration near the entrance. The mesh is also concentrated near the upper wall. The aspect radio of the grids plotted is different from the actual one. The radial dimension was increased to improve the visualization of results.

Figure (4) presents a comparison of present results, for the radial profiles of the axial velocity component at four different axial stations, with experimental data of Chaturverdi (1963) and numerical data of Coelho et al. (1998), for

two different grid arrangements. The axial velocity, normalized by the mean inlet velocity (U_{in}), is plotted against the radial coordinate, normalized by the radius of the pipe downstream of the expansion. The analyses of profiles show that there is a good agreement between the experimental data and the results obtained with the present code. Even the redevelopment of the flow downstream of the reattachment point, which usually is slower in the numerical simulations using κ–ε turbulence model in according to literature data is closer to experimental data.

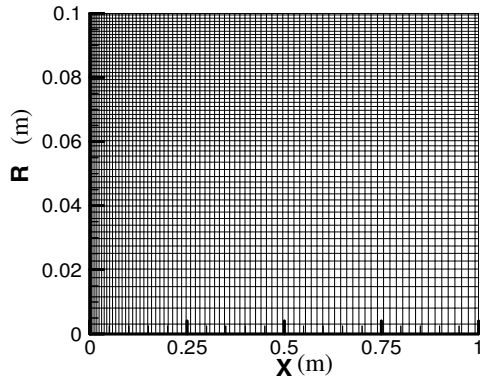

Figure 3. Grid used to compute the turbulent flow through a sudden pipe expansion.

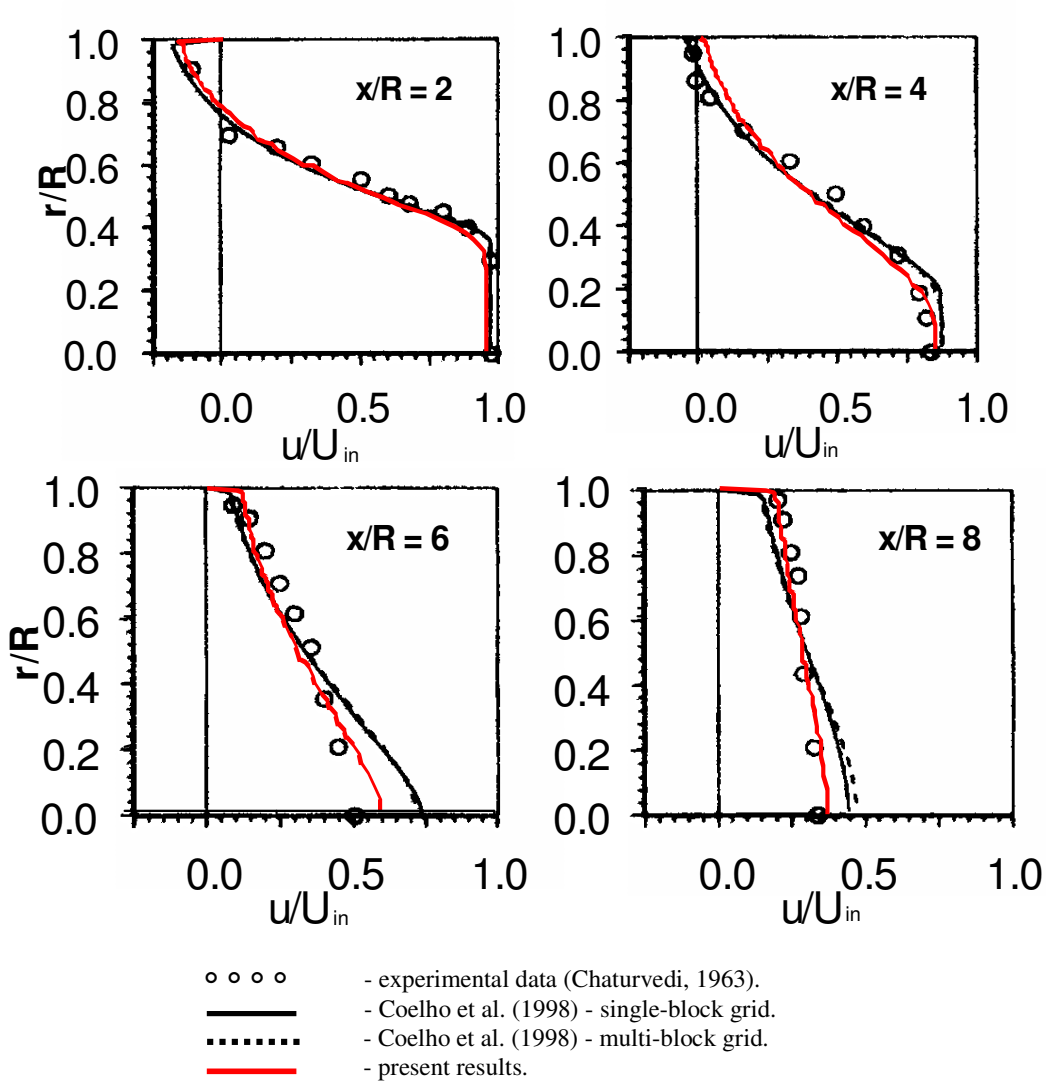

Figure 4. Predicted and measured radial u-velocity profiles for the flow through a sudden expansion.

In this case there is no chemical reaction; therefore differences between the Coelho et al. (1998) model and the present model are the wall function and the boundary condition of the turbulent kinetic energy at the walls. The wall function method of Chieng and Launder (1980) was used by Coelho et al (1998). With this method, the κ values at a grid node close to the wall were calculated by solving its transport equation, with production and destruction terms replaced by available expressions in accordance with assumed profile for the variable within the boundary layer. At the present paper the traditional law of the wall by Launder and Spalding (1976) was employed, where the κ values at grid node close to the wall were calculated by solution of the same transport equation as the core region, without simplifying the production and destruction terms.

5.2 Reactive flow in a solid fuel combustion chamber of a ramjet

The flow field inside a solid fuel combustion chamber of a ramjet is investigated next. The solution obtained with the proposed model is compared with available experimental (Elands et all, 1990) and numerical (Coelho et all, 1998) data. The combustion chamber has a length of 0.3 m. The inner diameter of the combustion chamber increases along the time due to fuel (polyethylene) pyrolysis, but this process was not taken into account by the proposed model. The fuel grain diameter was set equal to 45 mm for calculation purposes. This is an average value of the inner diameter during combustion, when the measurements were carried out. Air at a temperature of 300 K and a pressure of 0.40 MPa is admitted into the combustion chamber through a port of 15 mm diameter. The air flow rate is 150 g/s.

Calculations were performed using a non-uniform computational grid with 82×62 nodes shown in the Fig. (5). Again, the radial dimension was increased to improve the visualization of results.

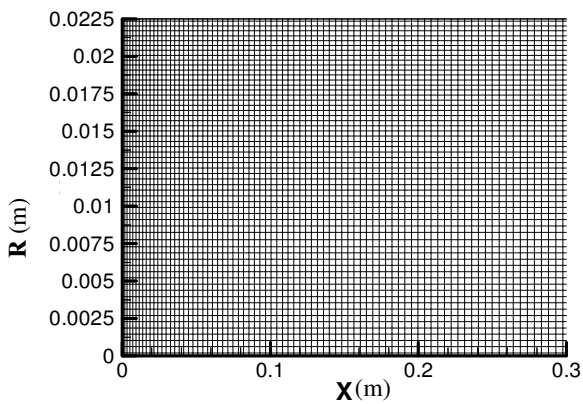

Figure 5. Grid used to compute the flow in a solid fuel combustion chamber.

The temperature of the solid fuel surface was assumed constant and equal to 700 K. The density of vaporized fuel was calculated by equation of state based on the pressure in the chamber and the solid fuel surface temperature.

For this case, since there is combustion, the transport equations for mixture fraction and variance of mixture fraction were included in the algebraic system. The solution of reactive flows is more difficult, due to the increase on the number of variables and especially due to the coupling of the density with flow variables. Therefore, under relaxation factors are fundamental for the convergence of the iterative procedure.

Figure (6) shows the predicted temperature and mixture fraction contours using the Coelho at al. (1998) model and the proposed model. The mixture fraction contours are very similar for the both models. Very low values of mixture fraction, characteristic of a lean mixture, are observed in the core of the combustor, and large values, typical of a rich mixture, are confined to a thin annular region close to the wall and the recirculation region just near the inlet of the chamber. The low blowing velocities at solid fuel surface explain this behavior. Because the amount of vaporized fuel injected in the flow is small, it is almost all burned as soon as it enters the flow and a small part is mixed and burned in the recirculation region. The agreement between predictions is good. The results for temperature contours are in close agreement to each other. The reaction zone corresponds to the region where higher temperatures occur. In the calculations a larger region with temperatures above 2100 K was obtained which extends to the region closer to the step at the inlet. The proposed model predicts a larger reaction zone and higher gradients near to the inlet region.

As in the previous case, predicted radial profiles of the normalized u-velocity component at four stations are plotted in Fig. (7). Since no experimental data is available for this problem, only predicted results are shown. The profiles obtained are similar, with larger differences occurring at the centerline, for stations far from the inlet section. The authors believe that the present results are a better prediction of the flow field. This statement can be made if one examines the previously obtained result in the Fig. (4). The profiles showed in that case also present differences in the region near to centerline. However, those results show a better agreement with experimental data.

The predicted evolution of the local mean regression rate along the fuel wall is plotted in the Fig. (8) along with the experimental data (Elands et all, 1990). The predicted regression rate increases significantly along the centerline up to the reattachment point, and decreases farther than previously downstream approaching a constant value. The Coelho et

all (1998) model and the proposed model over predicted the regression rate in the region of the flow upstream of the reattachment point and tend to underestimate the experiments that show only a very smooth peak. In accord to Elands et all (1990), the over prediction of the local mean regression rate in the recirculation region is attributed to the inability of the κ–ε turbulence model, together with the wall functions, to predict accurately the heat transfer behind a step. Since the regression rate is linearly related to the flux to the wall, the regression rate is affected by errors associated with the heat flux calculation.

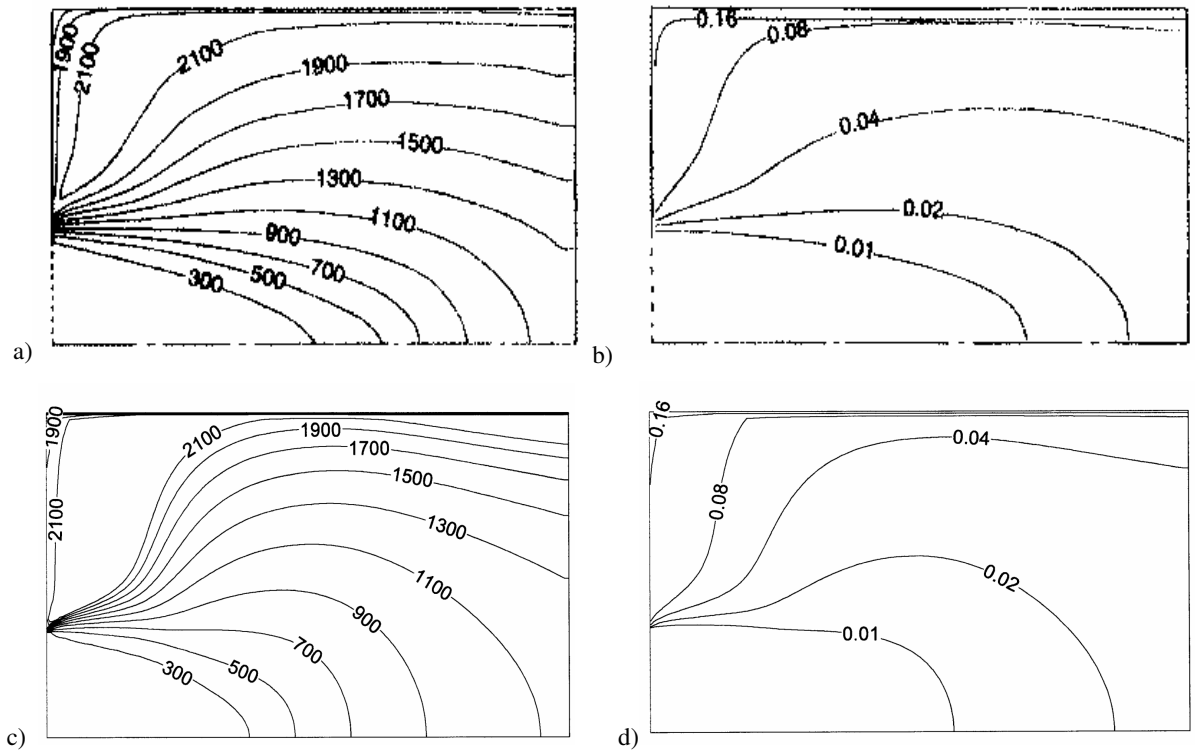

Figure 6. Predicted contours for the flow in a solid fuel combustion chamber. a) Temperature (K), Coelho at al. (1998). b) Mixture fraction, Coelho et al. (1998). c) Temperature (K), proposed model. d) Mixture fraction, proposed model.

The models yielded qualitatively similar evolutions of the local mean regression rate along the wall, but the proposed model predictions are consistently higher than the ones of Coelho et all (1998) model. However, all evolutions exhibit the shortcomings described above if compared to the experimental data, although the predicted results were in qualitative agreement with them.

The predicted evolution presented similar behavior after reattachment point, unlike the experimental behavior. It can be summarized that there is an important mechanism that was neglected. In accord to Methochianakis and Netzer (1983), radiant heat transfer must be included in the evaluation of heat flux to wall. This inclusion tends to decrease the difference between prediction and experimental results in the end portion of the chamber.

6. Conclusions

The results show that the model proposed for simulation of turbulent reactive flows in a solid fuel ramjet combustor is suitable. The evolution of the local regression rate was in qualitative agreement with experimental data. The observed discrepancies are mainly due to shortcomings of the turbulence model employed.

7. Acknowledgement

The authors acknowledge support from CNPq.

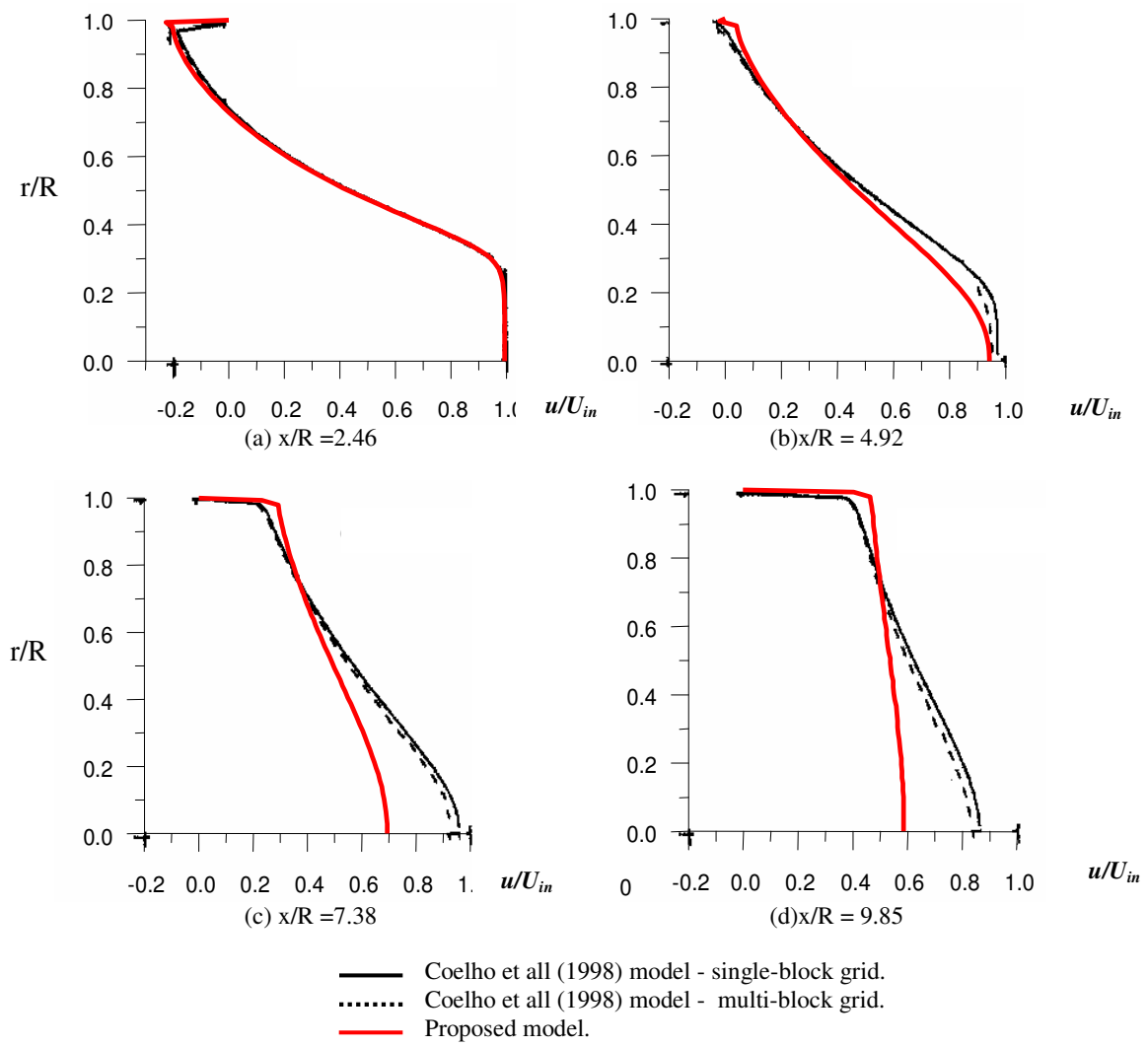

Figure 7. Predicted *u*-velocity profiles for the flow in a solid fuel combustion chamber.

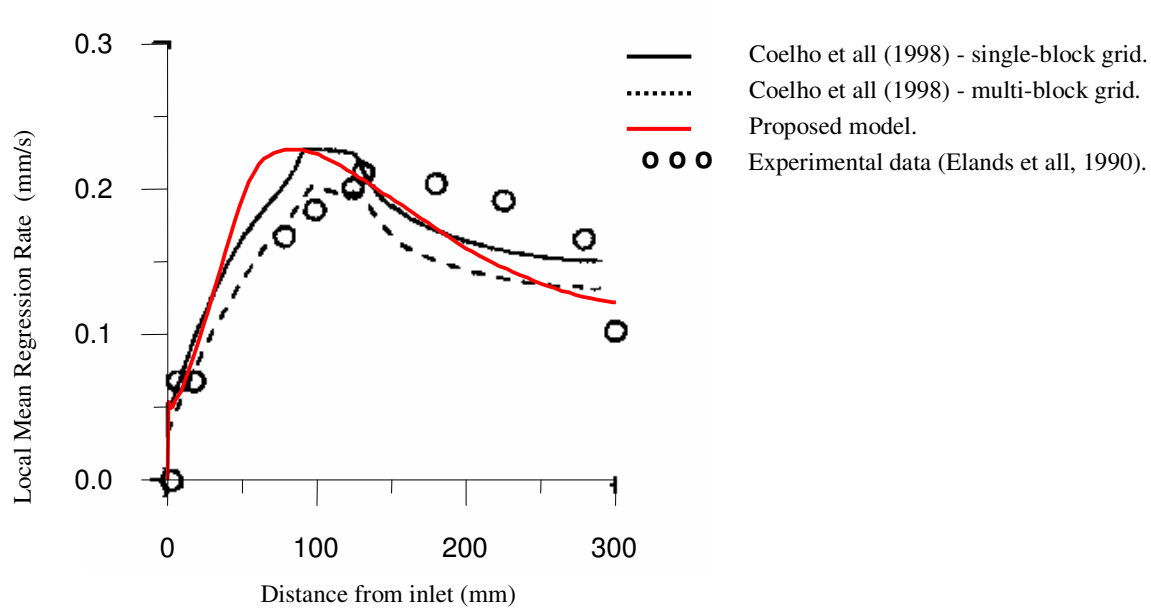

Figure 8. Predicted and measured regression rate along the wall.

8. References

Boaz, L. D., Netzer, D. W., 1973, "An Investigation of the Internal Ballistics of Solid Fuel Ramjets", Naval Postgraduate School, Rept. NPS-57NT73031a.

Chatuverdi, M. C., 1963, "Flow Characteristics of Axissymmetric Expansions", J. of the Hydraulics Division, Proc. ASCE, 89, pp. 61-92.

Chieng, C. C., Launder, B. E., 1980, "On the Calculation of Turbulent Heat Transfer Downstream from an Abrupt Pipe Expansion", Numerical Heat Transfer, 3, pp. 189-207.

Coelho, P. J., Duic, N., Lemos, C., Carvalho, M. G., 1998, "Modeling of a Solid Fuel Combustion Chamber of a Ramjet Using a Multi-block Domain Decomposition Technique", Aerospace Science and Technology, 2, pp. 107-119.

Elands, P., Korting, P., Wijckers, T., Dijkstra, F., 1990, "Comparison of Combustion Experiments and Theory in Polyethylene Solid Fuel Ramjets", J. Propulsion and Power, 6, pp. 732-739.

Kays, W. M., 1966, "Convective Heat and Mass Transfer", McGraw-Hill, pp. 300-313 and 326-328.

Launder, B. W., Spalding, D. B., 1973, "The Numerical Computation of Turbulent Flows", Computer Methods in Applied Mechanics and Engineering, pp. 269-289.

Metochianakis, M. E., Netzer, D. W., 1983, "Modeling Solid Fuel Ramjet Combustion Including Radiation to the Fuel Surface", Journal of Spacecraft and Rockets, Vol. 20, pp. 405-406.

Netzer, D. W., 1977, "Modeling Solid-Fuel Ramjet Combustion", Journal of Spacecraft, 14(12), pp. 762-766.

Patankar, S. V., 1980, "Numerical Heat Transfer and Fluid Flow", Hemisphere Publishing Corporation, Taylor and Francis Group, New York.

Settari, A. , Aziz, K., 1973, "A Generalization of the Additive Correction Methods for the Iterative Solution of Matrix Eq.", SIAM Journal of Numerical Analysis, Vol. 10, pp. 506-521.

Stevenson, C. A., Netzer, D. W., 1981, "Primitive-variable Model Applications to Solid-Fuel Ramjet Combustion", Journal of Spacecraft and Rockets, 18(1), pp. 89-94.

Wolfram, S. 2002, "The Mathematic Book", Cambrige University Press.

9. Copyright Notice

The authors are the only responsible for the printed material included in this paper.